Fault geometry and kinematics at the intersection of the Zemuhe, Daliangshan and Xiaojiang Faults

Mingming Wang[1], Zhanyu Wei[2]*, Feng Long[1], Han Chen[1] and Sheng Li[3]

[1]Sichuan Earthquake Agency, Chengdu, China, [2]State Key Laboratory of Earthquake Dynamics, Institute of Geology, China Earthquake Administration, Beijing, China, [3]Yunnan Earthquake Agency, Kunming, China

The complexity of strike-slip fault segmentation affects the initiation, propagation, and termination of earthquake ruptures and the earthquake magnitude. Studying the fault geometry, kinematics, and segmentation provides fundamental knowledge for mitigating earthquake hazards along faults. The Zemuhe, Daliangshan, and Xiaojiang Faults intersect along the eastern boundary of the Tibetan Plateau in the area from Ningnan in Sichuan Province to Qiaojia in Yunnan Province. Although few large earthquakes have occurred on these faults, the relationships between the intersections of these three faults and earthquake rupture behavior in this region are poorly constrained. The interpretation of aerial photographs and detailed field surveys revealed the geometric pattern and fault kinematics in the area of intersection. The distribution patterns and focal depths near the faults were obtained via analysis of seismic data in the area of intersection. The northern segment of the Xiaojiang Fault deviates approximately 25° northwest of Qiaojia, forming a conspicuous bend. The Xiaojiang Fault continues to extend southeast of the Ningnan Basin, where it intersects with the southern segment of the Zemuhe Fault, forming a pull-apart basin approximately 4.5 km wide. The bend and Ningnan pull-apart basin mark the segmented boundary between the Zemuhe Fault and the Xiaojiang Fault, which may prevent the propagation of large earthquake ruptures along the eastern boundary fault. Moreover, the lack of obvious geometric complexity between the Daliangshan Fault and Xiaojiang Fault might hinder the prevention of earthquake rupture propagation. Additionally, our results suggest that different earthquake prevention and disaster reduction measures should be taken for different cities in the region.

KEYWORDS

fault intersection area, geometric pattern, fault kinematics, earthquake rupture, Tibetan plateau

1 Introduction

The study of fault segmentation in active areas is highly important for quantitatively evaluating long-term seismic hazards (Aki, 1984; Wen, 2000). Geometrically discontinuous segments or complex fault patterns, such as steps (Harris and Day, 1993), bending structures (Nielsen and Knopoff, 1998) or branches (Andrews, 1994), are important marks representing fault rupture segmentation. As obstacles to strike-slip faulting, these features are segments of uneven stress distribution in the fault zone, which may affect the initiation,

FIGURE 1
Seismotectonic map of the study area.
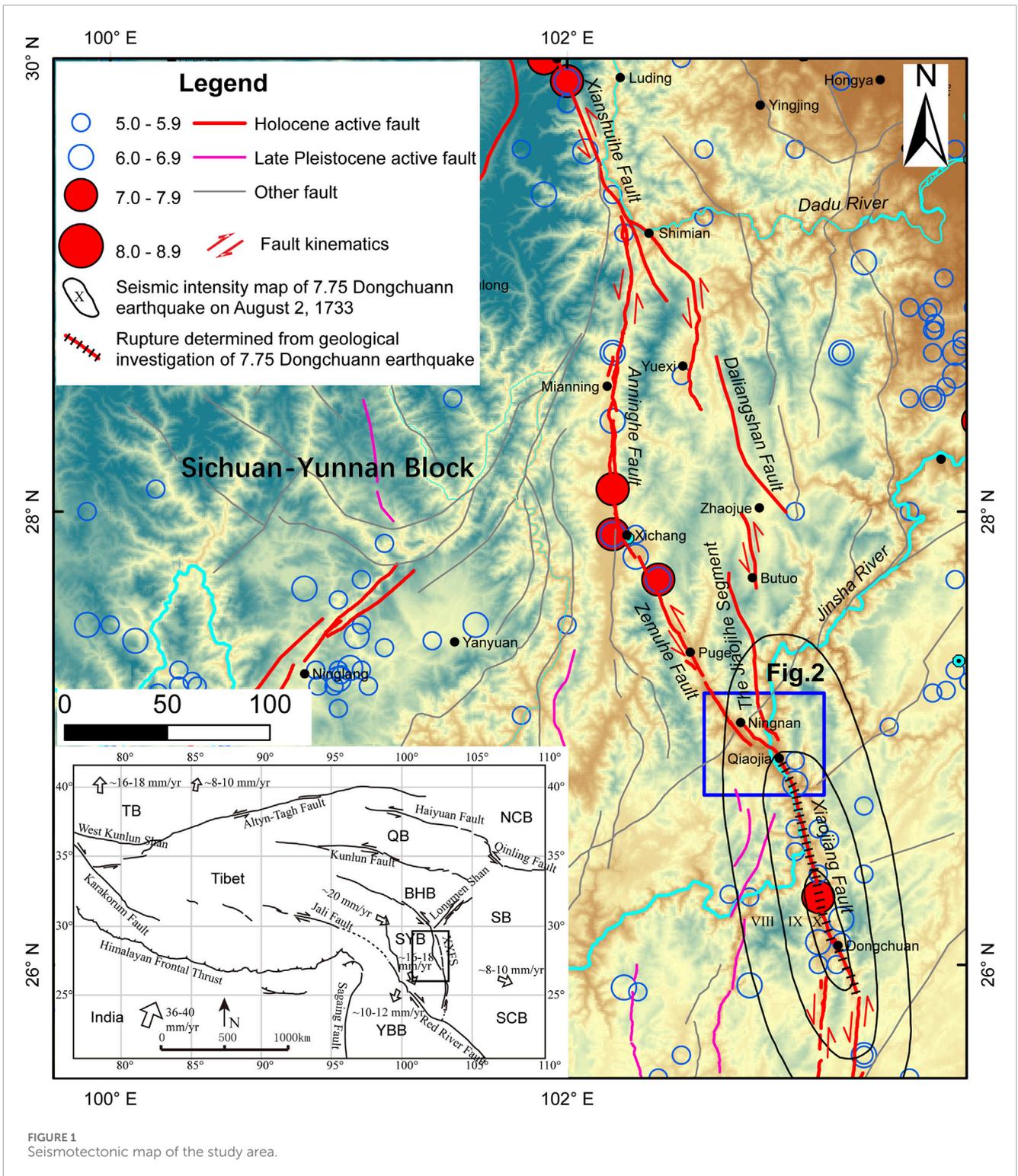
propagation and termination of earthquake rupture and the magnitude of the earthquake (Sieh et al., 1993; Hamling, et al., 2017; Jia et al., 2023). Depending on the size, geometry and type of movement of these barriers, they may become persistent or nonpersistent rupture boundaries for seismic propagation (Wesnousky, 2006).

The area of fault intersection is generally considered a geometric mark of fault segmentation, which can block the propagation of

earthquake ruptures to a certain extent, but there are also cases of strong earthquakes occurring, despite the segmentation. For example, destructive twin earthquakes (Mw 7.8–7.7) in 2023 ruptured multiple segments of the East Anatolian Fault System in Turkey, rupturing multiple geometrically complex segments, including fault intersections, bends, and steps (Jia et al., 2023), which were previously thought to be possible persistent rupture boundaries on the fault (Duman and Emre, 2013). Previous studies have focused primarily

TABLE 1 Summary of slip rates along the eastern boundary of the Sichuan–Yunnan Block.

Fault	Slip rate (mm/yr)	References	Method
XSH Fault	10–20	Allen et al. (1991)	Inferred age
	14–20	Chen et al. (2008)	Lower terrace age
	8–11	Zhang (2013)	Reinterpretation of Chen et al. (2008), using the upper terrace age
	6.5–12	Chevalier et al. (2017)	using their MGT ages along the Ganzi Fault
ANH Fault	3.6–6.2	Ran et al. (2008)	Lower terrace age
	5.5–7.5	Xu et al. (2003)	Lower terrace age
ZMH Fault	4.9	Ren and Ping (1989)	Lower terrace age
	5.8–8.5	He et al. (1999)	Lower terrace age
DLS Fault	2.6–3	Rongjun et al. (2003)	Lower terrace age
	2.5–4.5	Zhanyu et al. (2012)	Lower terrace age
XJ Fault	8–12	Song et al. (1998)	Lower terrace age
	13–16.5	He et al. (2002)	Lower terrace age
	7.02	Han et al. (2017)	Lower terrace age

FIGURE 2
Geometric pattern and distribution of survey points in the area of fault intersection.
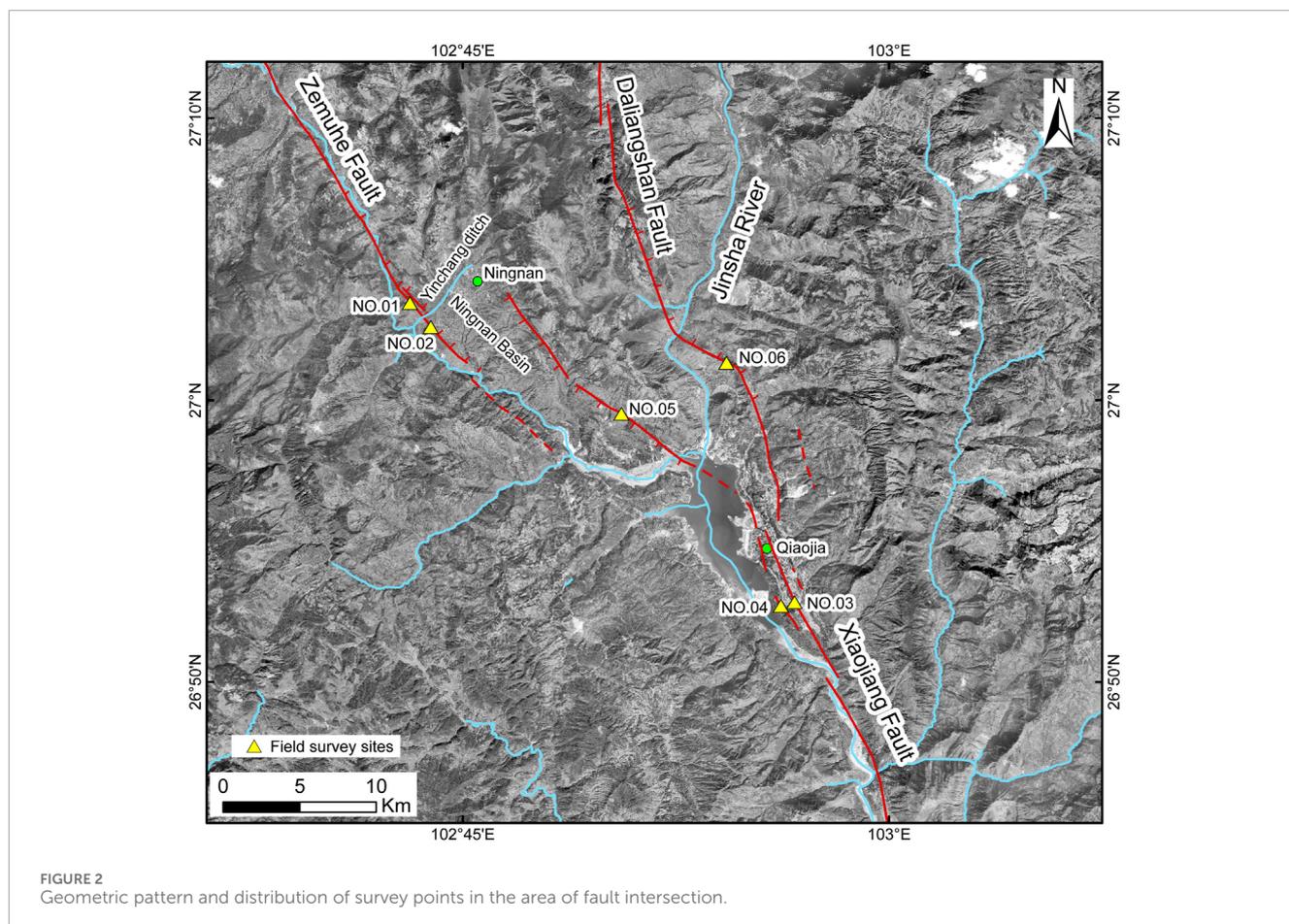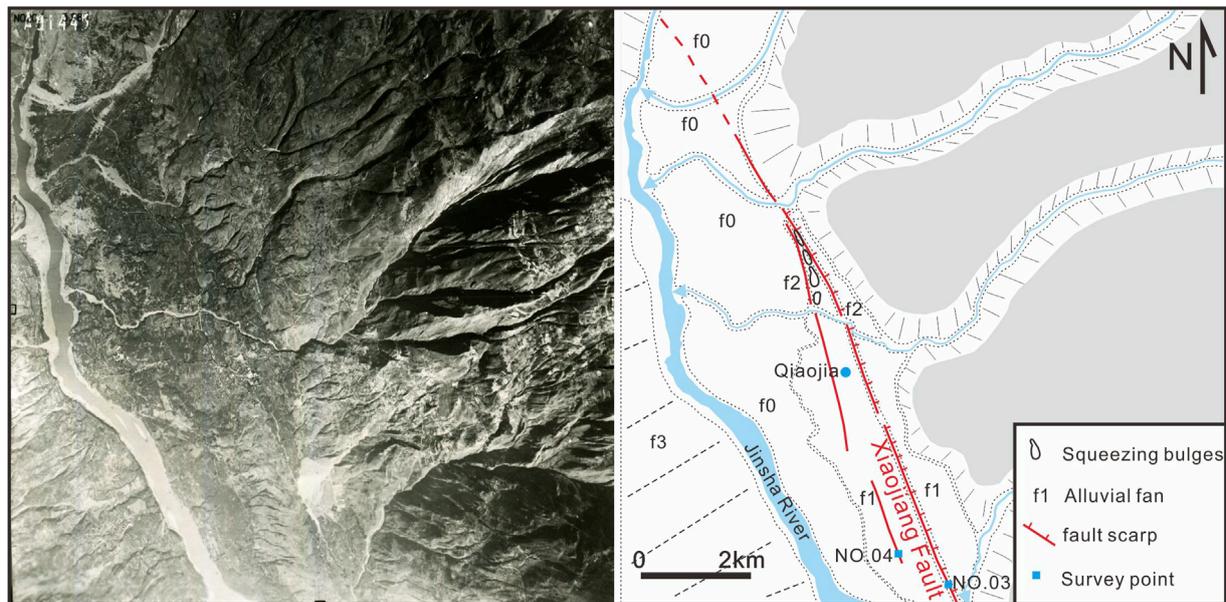
FIGURE 3
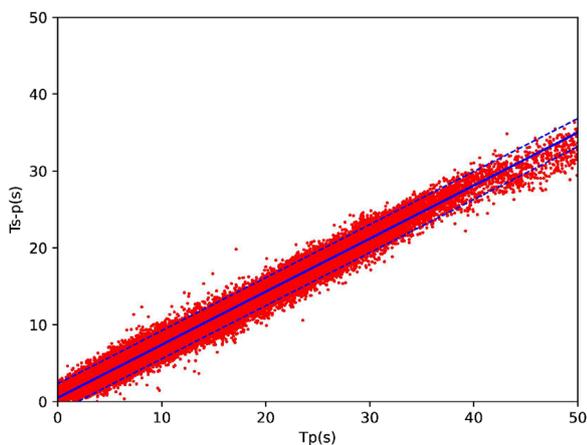Aerial photographs and interpreted maps near Qiaojia County.

FIGURE 4
Phase data selection based on the Wadadi diagram The blue solid line indicates the fitted mean value, and the dashed lines represent the $\pm 3.0\sigma$ threshold lines.

on the effects of fault geometry on the propagation of earthquake ruptures at fault step locations (Shao et al., 2018; Bai et al., 2018), with relatively few studies conducted on the areas of intersection of multiple branching faults (Zhao et al., 2022).

The Sichuan–Yunnan Block, bounded by the Xianshuihe–Xiaojiang Fault System to the east and the Jinshajiang–Red River Faults to the west, is one of the most tectonically and seismically active blocks in the southeastern Tibetan Plateau (Figure 1). Historically, approximately 37 strong earthquakes with magnitudes greater than six have occurred along the eastern boundary faults (Wen et al., 2008), and the latest Ms 6.8 earthquake

occurred near Shimian in 2022 at the area of intersection of the Xianshuihe, Anninghe and Daliangshan Faults (Yi et al., 2023). Several intersections have developed in the eastern boundary fault system of the Sichuan–Yunnan Block. Among these complex features of strike-slip faults along the eastern boundary, the Ningnan–Qiaojia partition zone can be identified as a persistent obstacle at the end of the Zemuhe Fault (Wen, 2000). Moreover, detailed mapping has been carried out in this area, and previous scholars have noted that the segmentation of the three faults is near the Jinsha River. However, insufficient comprehension of geometric patterns and fault kinematics based on the fault system makes it unclear whether this zone is the persistent boundary of ruptures from the propagation of seismic activity, resulting in great uncertainty in assessing seismic hazards and understanding the mechanisms of propagation of major earthquakes in the area of intersection.

Focusing on these problems, a field investigation was carried out on the basis of detailed aerial photograph interpretation, and then, the source data of earthquakes were analyzed through accurate relocation of the 5744 earthquakes in the area of intersection to provide valuable examples for the analysis of strike-slip fault segmentation. Additionally, this research can serve as a good reference for seismic hazard assessments in the region and is crucial for guiding strategies for active fault avoidance in cities along faults.

2 Geological and seismotectonic setting

The Anninghe–Zemuhe–Xiaojiang Fault System, as the eastern boundary fault system of the Sichuan–Yunnan Block (Figure 1), regulates the sinistral strike-slip movement resulting from the collision of the Eurasian Plate, leading to southeastward extrusion of the Qinghai–Tibetan Plateau (Tapponnier and Molnar, 1977;
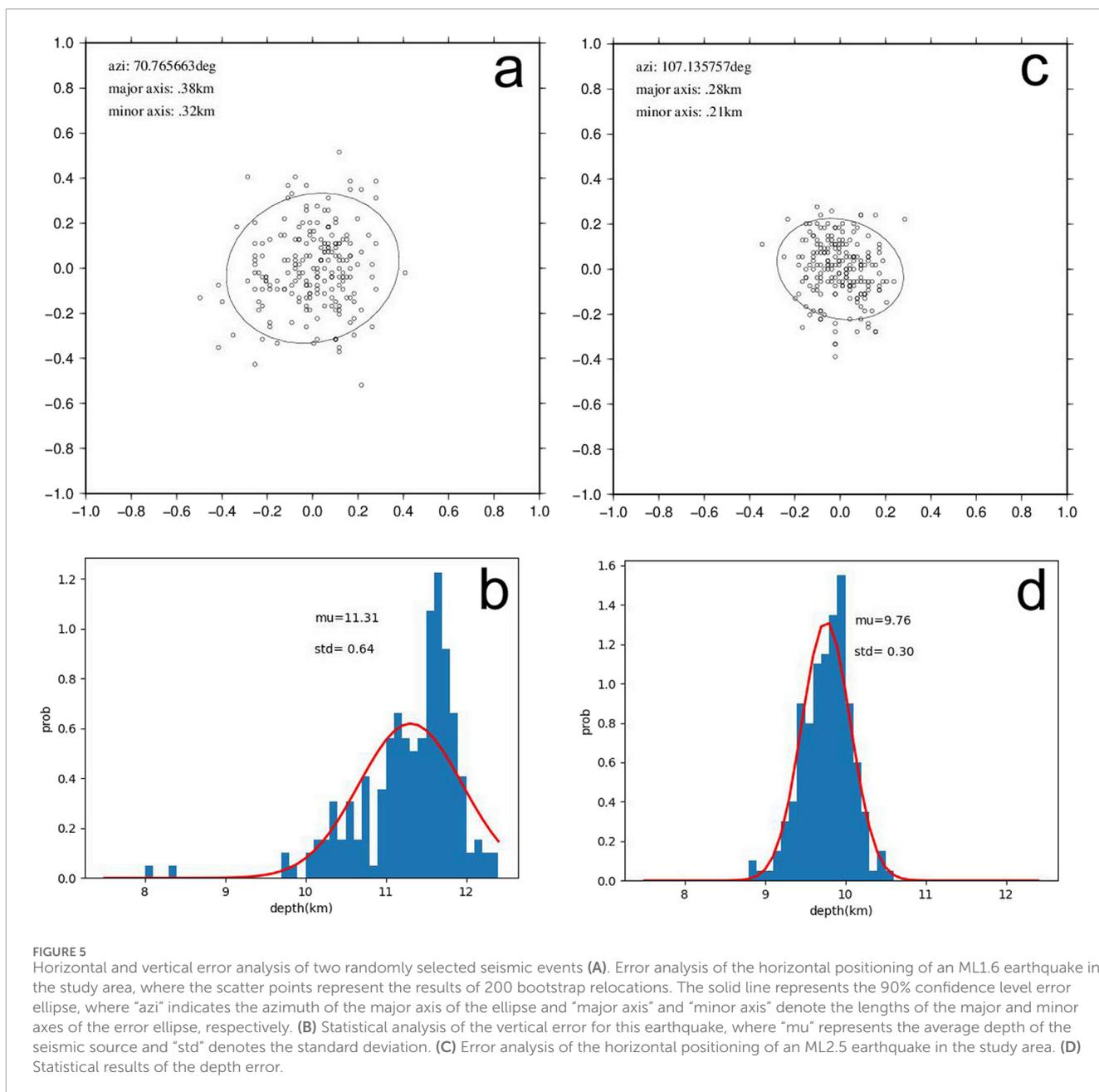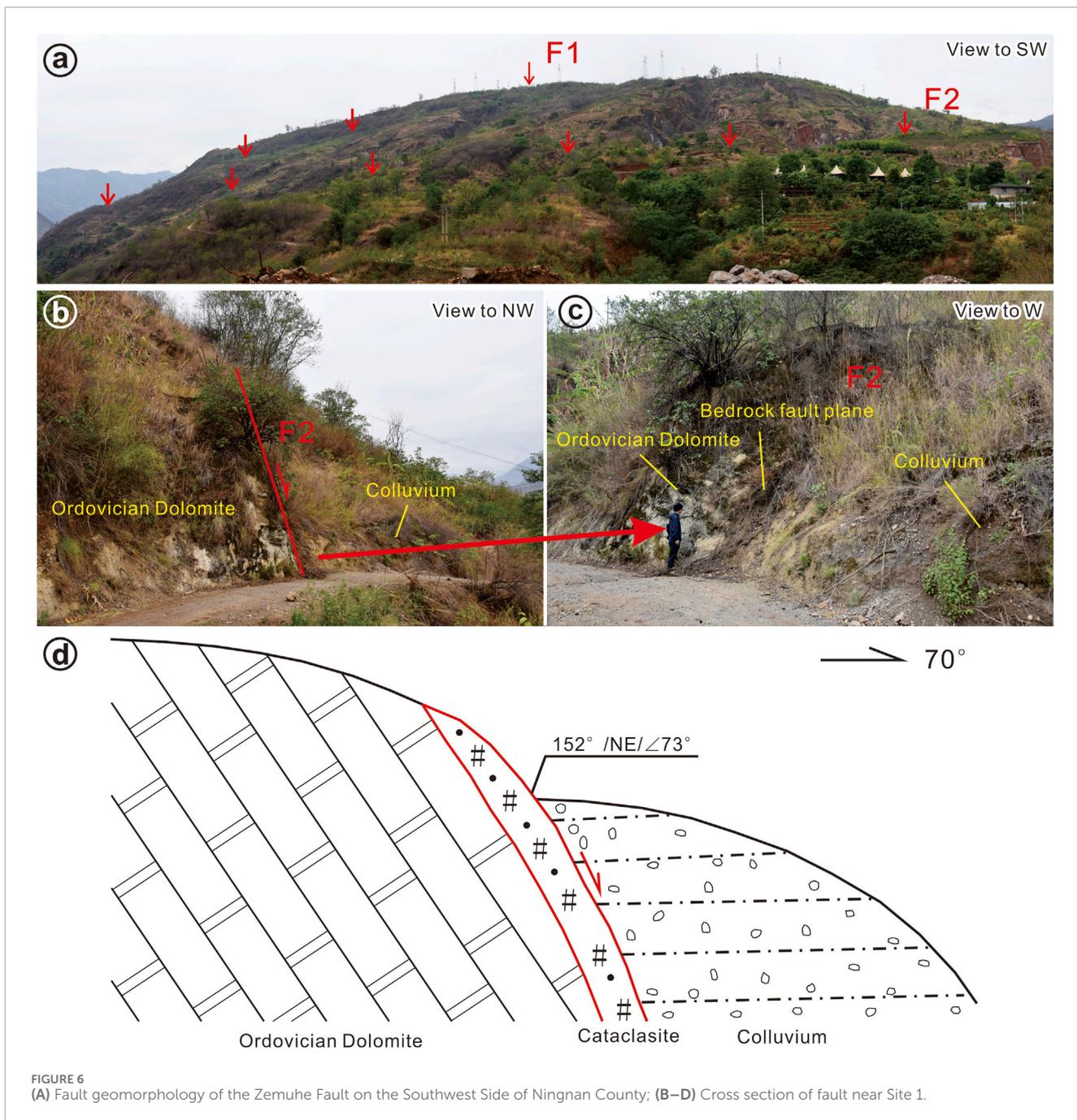
FIGURE 5
Horizontal and vertical error analysis of two randomly selected seismic events **(A)**. Error analysis of the horizontal positioning of an ML1.6 earthquake in the study area, where the scatter points represent the results of 200 bootstrap relocations. The solid line represents the 90% confidence level error ellipse, where "azi" indicates the azimuth of the major axis of the ellipse and "major axis" and "minor axis" denote the lengths of the major and minor axes of the error ellipse, respectively. **(B)** Statistical analysis of the vertical error for this earthquake, where "mu" represents the average depth of the seismic source and "std" denotes the standard deviation. **(C)** Error analysis of the horizontal positioning of an ML2.5 earthquake in the study area. **(D)** Statistical results of the depth error.

Wang et al., 1998; Wang and Burchfiel, 2000). As a part of the eastern boundary of the Sichuan–Yunnan Block, the Anninghe–Zemuhe Fault and the Daliangshan Fault form a segment that bends between the Shimian and Qiaojia regions, with a width of approximately 100 km and a length of approximately 300 km. This bend intersects with the Xianshuihe Fault to the northwest and the Xiaojiang Fault to the southeast.

The distribution of slip rates on the eastern boundary faults reveals that the Xianshuihe Fault has relatively high slip rates of approximately 6.5–20 mm/a (Table 1; Allen et al., 1991; Zhang, 2013; Chevalier et al., 2017). This slip rate is distributed southward along the bend from Shimian to Qiaojia. The Anninghe–Zemuhe Fault and the Daliangshan Fault have approximately equal slip rates (Ren and Ping, 1989; He et al., 1999; Xu et al., 2003; Rongjun et al., 2003; Ran et al., 2008; Zhanyu et al., 2012), whereas the Xiaojiang

Fault to the south has slip rates of approximately 8–13.2 mm/a (Song et al., 1998; He et al., 2002; Han et al., 2017). Additionally, the Xiaojiang Fault exhibits a significant normal faulting component with a rate of extension of approximately 3.7 ± 0.2 mm/a in the central-southern segment (Wang et al., 2021).

Owing to the high slip rate and intensity of activity of the Xianshuihe-Xiaojiang Fault System, its seismic capacity and earthquake hazard in the area are both relatively high, leading to frequent moderate earthquakes. Within the research area, the northern segment of the Zemuhe Fault produced a 7.5 magnitude earthquake near Xichang on 12 September 1850, and two earthquakes of magnitude 6.75 occurred in 1489 and 1732. Additionally, the northern segment of the Xiaojiang Fault produced a 7.75 magnitude earthquake near Dongchuan on 2 August 1733 (China Earthquake Administration, 1995). Although there are no

FIGURE 6
(A) Fault geomorphology of the Zemuhe Fault on the Southwest Side of Ningnan County; **(B–D)** Cross section of fault near Site 1.
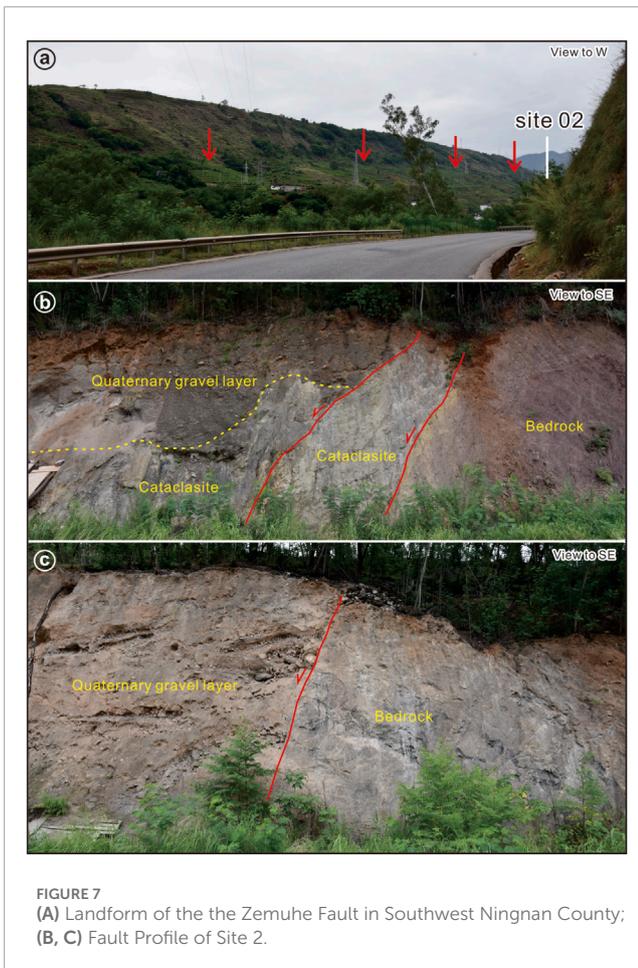
historical earthquake records along the Daliangshan Fault, Sun et al. (2019) and Li et al. (2020) revealed through paleoseismic studies, deformation data, and seismological data that the Jiaojihe segment of the southern segment of the Daliangshan Fault has accumulated energy capable of generating a Mw 7.5 magnitude earthquake, indicating a high earthquake hazard in the southern segment of the Daliangshan Fault.

In a study of segmentation from seismic ruptures in the Anninghe–Zemuhe Fault Zone, Wen (2000) identified two persistent segment boundaries at both ends of the Zemuhe Fault, namely, the Xichang Bend Zone and the Ningnan–Qiaojia partition zone. Within the Ningnan–Qiaojia partition zone, with a width of approximately 20 km, northeast-trending extensional

faults, northwest-trending normal–strike-slip faults, and two small late Quaternary basins, the Ningnan and Qiaojia Basins, are present (Wen, 1983). Owing to the lack of detailed studies on active faults in the area of intersection, the understanding of the characteristics of geometric patterns and intersecting relationships of active faults in the Ningnan–Qiaojia region is still insufficient.

3 Methodology and data

The main approach in this study combines aerial photograph interpretation with field investigations to explore the geometric pattern, fault movement, and intersecting relationships of the

FIGURE 7
(A) Landform of the the Zemuhe Fault in Southwest Ningnan County; **(B, C)** Fault Profile of Site 2.

avoid the interference of misidentified outliers on the positioning accuracy (Figure 4).

2. We initially located the events via HYPOINVERSE 2000 (Klein, 1989), with a velocity model of western Sichuan by Zhu and Zhang, (1987)bib_zhu_and_zhang_1987. From the preliminary location results, we selected observation reports of events with records from six or more stations and azimuthal gaps less than 150°. VELEST (Kissling, 1988; Kissling et al., 1994; 1995) was then employed to study the local minimum one-dimensional velocity model and station corrections in the study area.

3. The inverted velocity model and station corrections that were obtained were then re-entered into HYPOINVERSE2000 for relocation.

4. Finally, a double-difference relocation (Waldhauser and Ellsworth, 2000) was applied with a search radius of 10 km to correct the hypocenter positions.

Five hundred seismic events were randomly selected, and 200 bootstrap analyses for each event were conducted. The statistical results revealed average positioning errors of 800 m horizontally and 1500 m vertically (Figure 5). During the double-difference relocation process, the positions of lost seismic events were replaced by the results from HYPOINVERSE 2000.

Through the analysis of the geometric patterns, kinematic properties, distributions and hypocenters of small earthquakes in the area of fault intersection, we further combined the rupture distributions of the 7.75 magnitude earthquakes in Dongchuan in 1733. Moreover, we propose a geometric segmentation scheme for the area of the Zemuhe–Daliangshan–Xiaojiang Fault intersection.

4 Geometric pattern and characteristics of fault activity

4.1 Zemuhe Fault

The Zemuhe Fault is connected to the Anninghe Fault Zone to the north; the fault starts from Xichang in the northwest, extends southeast through Puge to near Ningnan, and crosses the Ningnan Basin to the Xiaojiang Fault Zone, with a total length of approximately 110 km (Wen, 1983). The NNW-striking fault has a consistent trend overall. Since the late Quaternary, fault deformation has manifested mainly as left–lateral strike-slip movement, followed by extensional fault movement.

The Ningnan Basin is present at the end of the Zemuhe Fault. Two branch faults of the Zemuhe Fault have developed in the piedmont on the southwest side of the basin, manifesting as two nearly parallel fault scarps (site 1, 102°43′12.54″E, 27°3′24.87″N; Figure 6A). Faulted colluvium strata are observed in the profiles across the fault scarp (Figures 6B–D). The Zemuhe Fault trends northeast and exhibits extensional kinematic properties.

Cutting across the Yinchang gully, the fault continues to extend southeastward, manifesting as well-defined linear bedrock scarps. At the outcrop of the fault, two sets of nearly parallel fault planes can be observed (site 2, E 102°43′51.68″, N 27°2′35.24″; Figure 7). The main fault acts as the boundary between the bedrock and the Quaternary strata, and the Quaternary strata are faulted.

Zemuhe Fault, the Daliangshan Fault, and the Xiaojiang Fault in the target area. Owing to the construction of the Baihetan hydropower station on the Jinsha River, large areas of Qiaojia and Ningnan have been submerged by the reservoir, and large-scale development and construction have occurred in Qiaojia County. These factors have limited our study of the geological and geomorphological characteristics of the area of fault intersection (Figure 2). Therefore, we collected aerial photographs taken in the 1970s and 1980s and conducted detailed interpretation work on aerial photographs to obtain the fine geometric patterns of the three faults before the reservoir was filled (Figure 3). On the basis of clarifying the geometric patterns of the three faults, we conducted field investigations of the target faults and obtained the kinematics of the three faults through field geological profiles, thereby analyzing the relationships of intersection among them.

In this study, P-wave and S-wave phase time data were collected from 5744 earthquakes with magnitudes greater than $M_L 1.5$ recorded by the Sichuan Seismic Network from 2009–December 2022. A "multistage positioning method" (Long et al., 2015) was employed to locate these earthquakes precisely. The technique involved the following steps.

1. First, we selected data within the Wadadi diagram that were 3.0 times the average standard deviation to

FIGURE 8
(A) Fault geomorphology of site 3 on the Xiaojiang Fault near Qiaojia County; **(B)** Fault plane of the site 3.

FIGURE 9
(A,B) Profile of Site 4 on Xiaojiang Fault Branch Fault near Qiaojia County.
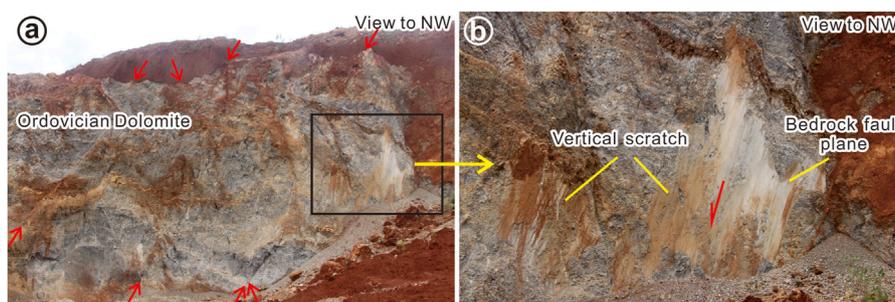
FIGURE 10
(A) Fault plane at Site 5 in Southeast Ningnan County; **(B)** vertical striation.
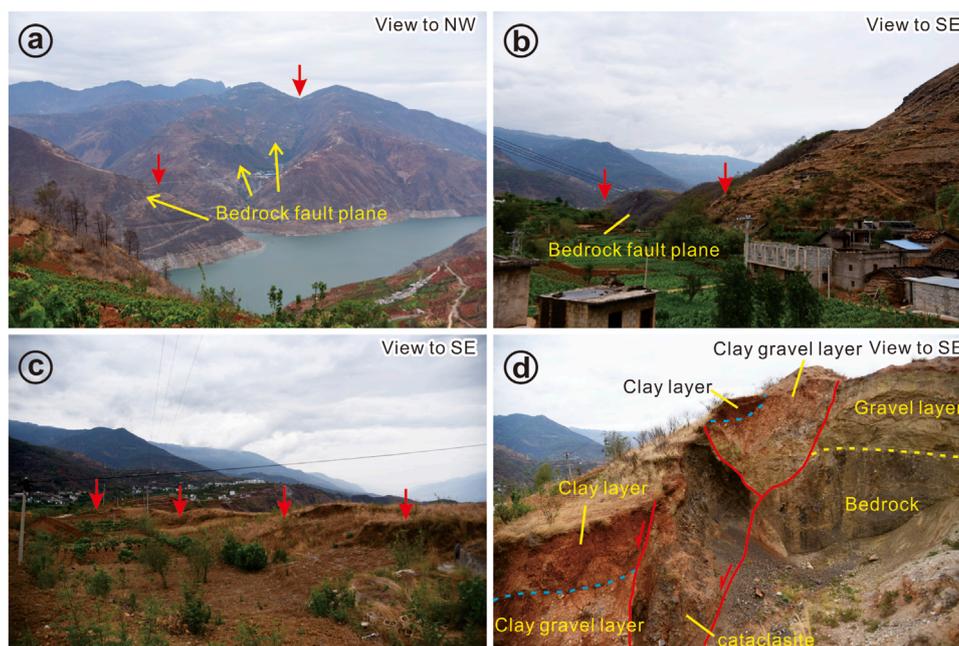
FIGURE 11
(A–C) The Geomorphic Features of the Daliangshan Fault on the South Bank of the Jinsha River; **(D)** Fault Profile of Site 6.

Branch faults have developed both within the bedrock and within the Quaternary strata, exhibiting overall extensional kinematic properties.

4.2 Northern segment of the Xiaojiang Fault

The middle–northern segment of the Xiaojiang Fault, which is the Dongchuan boundary, can be divided into northern and southern sections. From Dongchuan to Qiaojia, a single fault extends approximately 75 km (Figure 1). It mainly appears in the valleys of the Jinsha River and Xiaojiang River and features sinistral strike-slip and reverse steep scarps. Toward southern Dongchuan, the fault branches into two segments with widths of approximately 15 km. The western branch is the surface rupture zone of the 1833 M8 Songming earthquake, whereas the eastern branch corresponds to the surface rupture zone of the 1733 M7.75 Dongchuan earthquake (He et al., 2002).

Through aerial photograph interpretation, two fault planes can be observed near Qiaojia in the northern segment of the Xiaojiang Fault Zone, primarily exhibiting characteristics of sinistral strike-slip and extensional movement. The main fault manifests topographically as a northeast-trending reverse trough valley, displaying well-defined linear features. Along the Fault Zone, several springs have formed, and clear bedrock fault surfaces can be observed at excavation sites (site 3, E 102°56′41.97″, N 26°52′42.60″; Figure 8).

Furthermore, on the western side of the main fault, a synthetic fault plane can be observed within the alluvial fan, characterized by faulted gravel layers (site 4, E 102°56′11.24″, N

26°52′43.45″; Figure 9). This fault developed within the early to middle Pleistocene gravel layers, and due to the lack of exposed overlying strata, the most recent period of activity of this fault plane remains unclear.

The fault extends northwestward across the Jinsha River north of Qiaojia County town, with its trend shifting from north–northwest to northwest, with an approximate deviation of 25°. On the southeast side of Ningnan County, an approximately 80-m-wide fault–fracture zone is visible, within which multiple fault planes have developed (site 5, E 102°51′28.80″, N 26°58′51.37″; Figure 10). Vertical striations are also visible on the exposed portions of the fault fracture zone. The fault manifests as a southwest-dipping normal fault, indicating that the kinematics of the Xiaojiang Fault at this location exhibit a prominent normal fault component.

4.3 The Daliangshan Fault

The Daliangshan Fault starts from near Shimian in the north and extends southward through Yuexi, Puxiong, Zhaojue, and Buto to join the Xiaojiang Fault Belt in Qiaojia, with a total length of approximately 280 km (Figure 1). The Daliangshan Fault is a young fault belt that plays a role in "shortcutting" the middle section of the Xianshuihe–Xiaojiang Fault System and consists of six oblique branch faults. From north to south, they are the Zhuma Fault, Gongyihai Fault, Yuexi Fault, Puxiong Fault, Butuo Fault, and Jiaojiehe Fault (He et al., 2008). Among them, the Butuo Fault and Jiaojiehe Fault in the southern segment exhibit dextral stepped fault distributions, with lengths of 60 km and 70 km, respectively (Zhanyu et al., 2012). The geometric pattern and kinematics of the
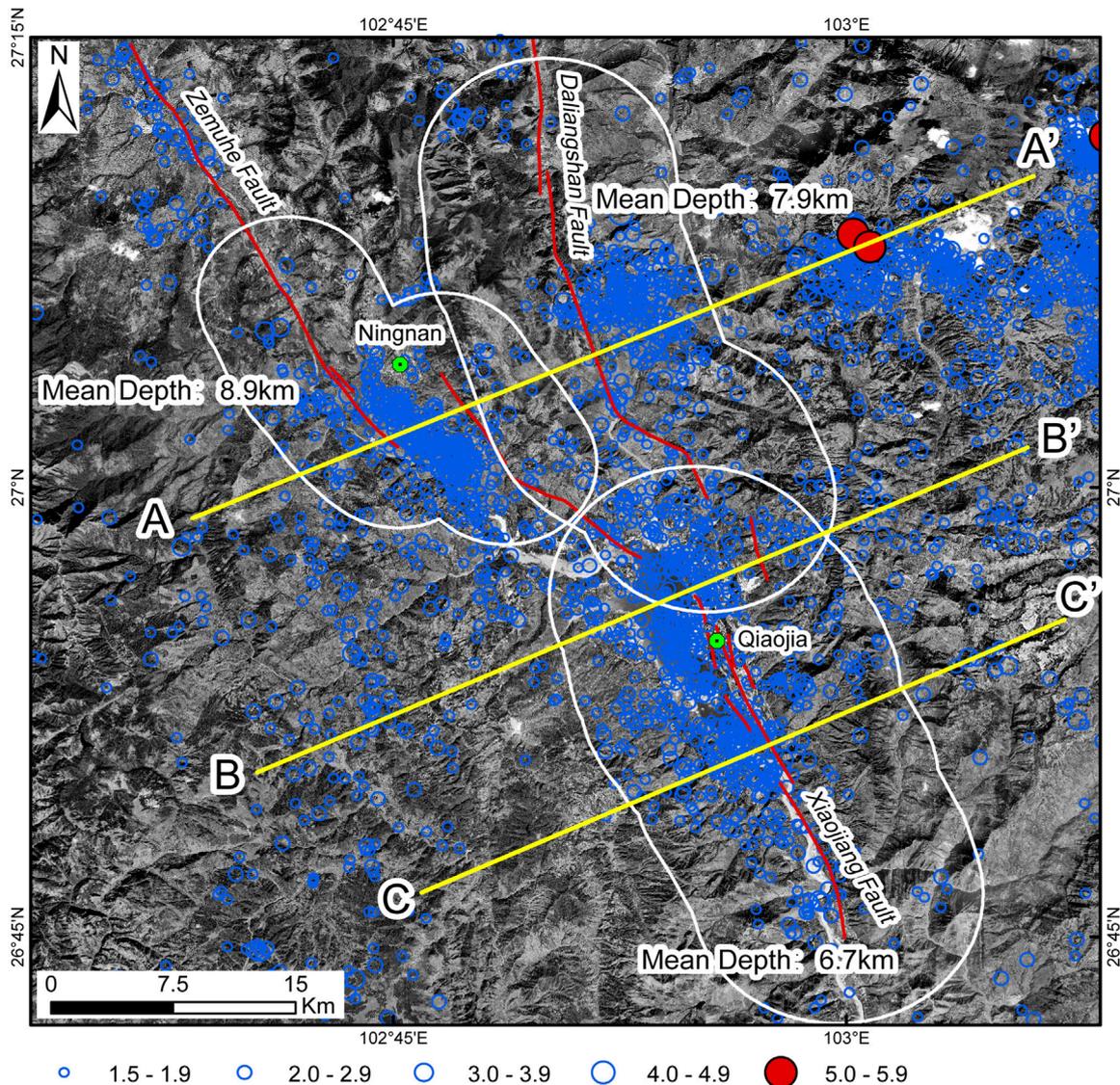
FIGURE 12
Distribution of small earthquakes and source depths along the fault in the study area.

Jiaojiehe Fault, as it crosses the Jinsha River to the south, are still open issues to explore (Figure 2).

The movement of the southern segment of the Jiaojiehe Fault is characterized by both strike-slip faulting and normal faulting. On the northern bank of the Jinsha River, the Jiaojiehe Fault shows northeastward-trending extension with tensile motion. The triangular facets of the fault are exposed, extending continuously to the southern bank of the Jinsha River (Figures 11A–C). At the point at which the Jiaojiehe Fault trend turns, the profile of the late Quaternary reddish-brown clay layer that is cut by the fault is visible (site 6, E 102°54′17.77″, N 27°1′19.92″; Figure 11D). From the point of the bend southward to the Qiaojia vicinity, the fault gradually diminishes in size.

Field surveys provide support for revealing the geometric distributions of faults and provide important information for understanding the characteristics of fault activity in this area. First,

through interpretation of aerial photographs, the geometric patterns of three faults were analyzed, on the basis of which, a field survey was carried out. As a consequence, fault profiles on all three faults and their branching faults were observed via field surveys, which confirmed that the fault positions interpreted from aerial photographs are accurate, providing a solid foundation for revealing the geometric fault pattern in the area of intersection. Second, vertical faulting can be observed in the field sections of the Zemuhe Fault and Daliangshan Fault, and even vertical striations can be observed on the fault Xiaojiang Fault plane. This demonstrates significant normal faulting components in the kinematics of the three faults in the intersection zone, indicating an extensional tectonic zone. The results provide a basis for revealing the kinematics of faults in areas of intersection. Third, both the Xiaojiang Fault and the Zemuhe Fault have branching faults, as shown in Figure 10. The fracture zone of the northern segment of the Xiaojiang Fault is
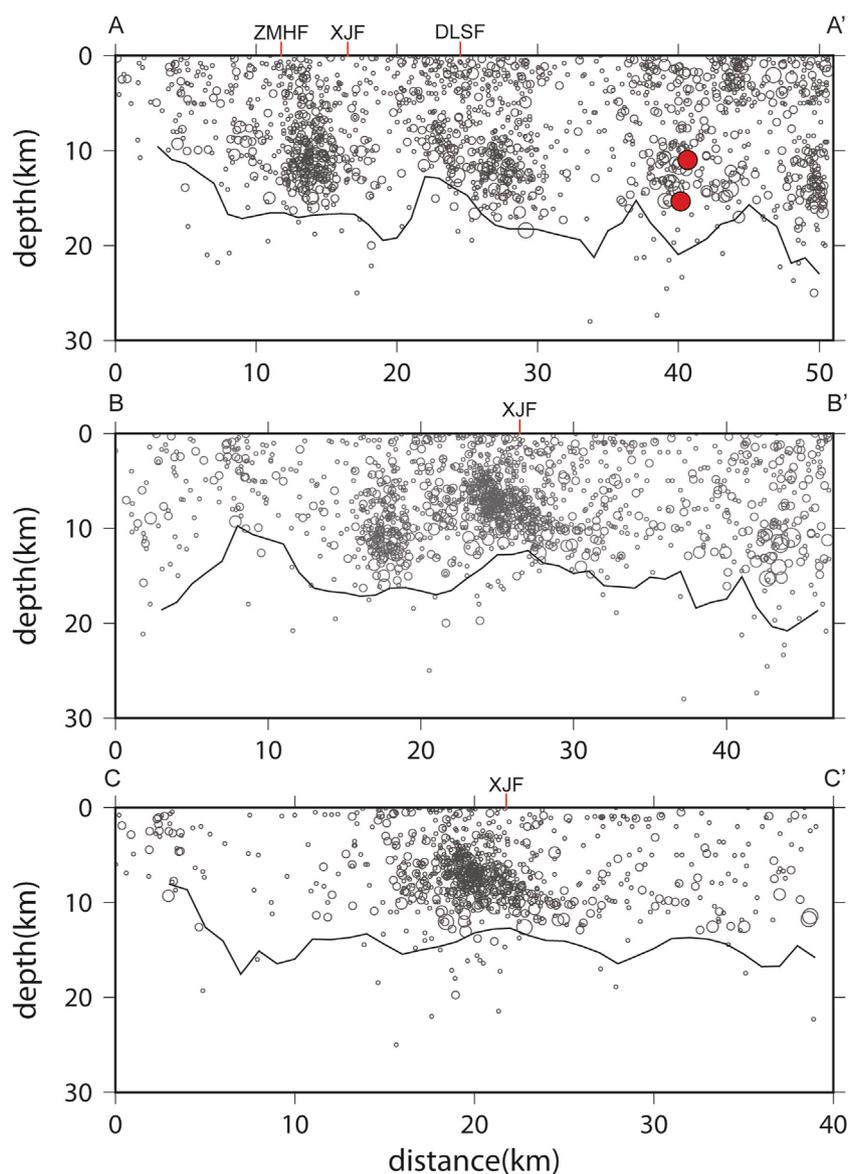
FIGURE 13
(A-A', B-B', C-C') denoted the cross-fault seismological profiles in the study area. The buffer zone is 10km on both side of the profile. The Gray line at the bottom indicates the depth at which 95% of the seismicity is above and 5% is below.

approximately 80 m long, which may be related to the complex stress at the fault intersection zone.

5 Earthquake sequence and seismogenic structure analysis

By accurately locating the small earthquakes in the study area, we obtained their distribution patterns and focal depths near the faults (Figure 12). Given that this area is where three faults intersect, to avoid interference from seismic data for other faults, we conducted statistical analyses and calculations of focal depths for small earthquakes within different ranges on either side of the faults. Specifically, near the Ningnan Basin, we conducted focal

depth statistics for small earthquakes within a 5 km range on either side of the fault. Similarly, at the Daliangshan Fault and Xiaojiang Fault locations, we selected small earthquakes within 7 km and 8 km ranges on either side of the faults, respectively, for focal depth statistics.

To further reveal the deep structural characteristics of the distribution of seismic activity along the faults, three cross-sectional lines, A-A′, B-B′, and C-C′, were designated, and earthquakes within a 10 km range were projected on either side of these lines (Figure 13).

The distribution and focal depth data of small earthquakes also confirm that the Ningnan Basin is a pull-apart basin with a width of approximately 4.5 km. Small earthquakes near the Ningnan Basin have occurred primarily between the boundary faults on either side
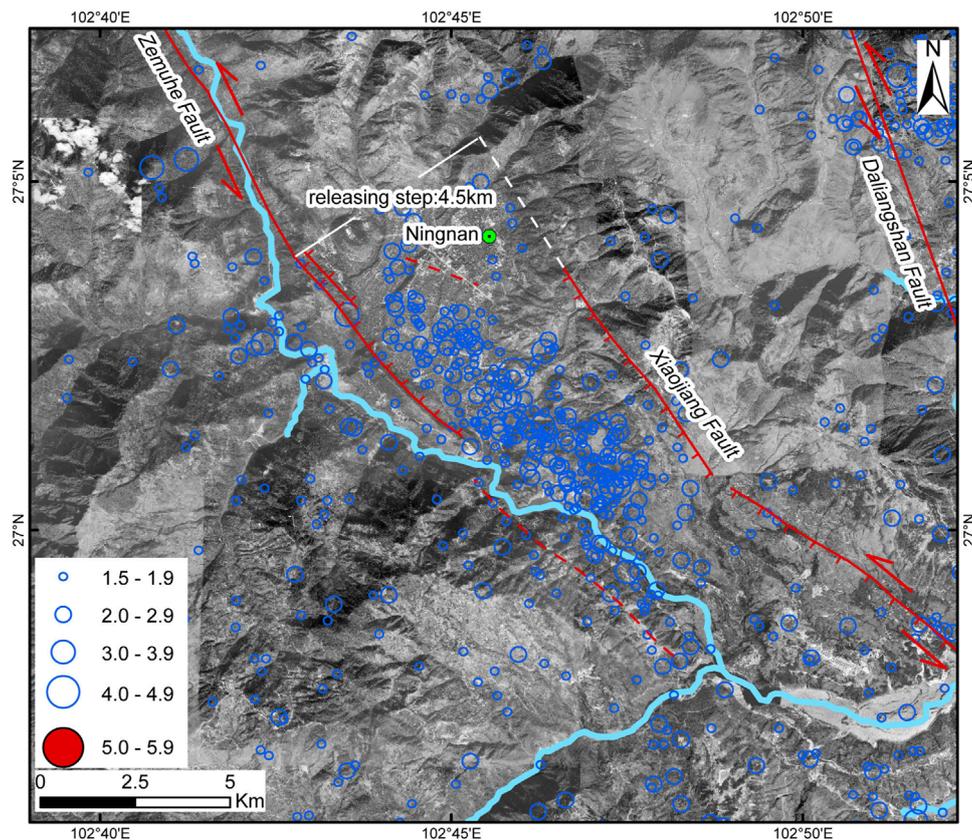
FIGURE 14
Distribution of faults and small earthquakes near the Ningnan Basin.

of the basin. This graben is formed by the left-step extension and left-lateral movement of the Zemuhe Fault and the Xiaojiang Fault, both of which exhibit significant normal fault components on either side of the basin (Figure 14).

Focal depth profile A-A′ reveals that the Zemuhe Fault on the northwest side of the Ningnan Basin is a steeply dipping fault trending in the northeast direction. The focal depths of small earthquakes near the basin are relatively deep, with an average focal depth of 8.9 km, which is related to the tectonic movement of the pull-apart basin. Between Ningnan in Sichuan and Qiaojia in Yunnan, the Xiaojiang Fault undergoes a noticeable bend in its strike, deviating from NNW to NW and forming a bend segment of approximately 25°. Small earthquakes have occurred mainly on the west side of this bend of the Xiaojiang Fault, with relatively shallow focal depths averaging only 6.7 km in this area. Moreover, small earthquakes near the Daliangshan Fault occur primarily on the east side of the fault, with an average focal depth of 7.9 km.

6 Discussion

In a study on the segmentation of seismic ruptures along the Anninghe–Zemuhe Fault Zone, Wen (2000) suggested that the Ningnan–Qiaojia partition zone was a persistent boundary of the fault segment at the end of the Zemuhe Fault that regulated

the southward horizontal movement of the western block of the Xiaojiang Fault Zone by developing extensional fracturing and fault depression basins, whereas on the western side of the partition zone, localized compressional uplift regulated displacement from the western side of the Zemuhe Fault Zone. However, this work reveals, through detailed interpretation of aerophotographs and field surveys, that the northern segment of the Xiaojiang Fault deviates approximately 25° northwest of Qiaojia, forming a conspicuous bend structure. The fault continues to extend southeast of the Ningnan Basin, where it intersects with the southern segment of the Zemuhe Fault, forming a pull-apart basin approximately 4.5 km wide. The bend structure and Ningnan–Qiaojia pull-apart basin collectively constitute the Ningnan–Qiaojia pull-apart zone. Moreover, the Daliangshan Fault experiences a minor bend across the Jinsha River and gradually connects with the Xiaojiang Fault near Qiaojia, with no apparent barrier between the two.

From the perspective of segmentation from seismic ruptures, whether earthquakes can propagate through fault junction zones determines the magnitude and destructiveness of earthquakes. Wesnousky (2006, 2008) collected data from 22 strike-slip earthquakes worldwide, with rupture lengths ranging from 10 km to 420 km. His research results revealed that two-thirds of the termination points of surface ruptures of strike-slip faults were related to the fault step area or the fault trajectory termination

point, indicating a critical width (~4 km). Generally, strike-slip seismic propagation cannot pass through a step area of more than 4 km. Moreover, numerical simulation results show that when strike-slip faults have a turning point of more than 20°, the resulting structure would block seismic ruptures to varying degrees so that some fractures from seismic activity can pass through, whereas others cannot (Duan and Oglesby, 2005; Kame et al., 2003; Lozos et al., 2011). The Xiaojiang Fault and the Zemuhe Fault are obstructed by bends and pull-apart basins simultaneously, which could serve as boundaries of segments hindering the propagation of seismic ruptures, thereby impeding the spread of earthquake energy. In contrast, the connection between the Xiaojiang Fault and the Jiaojiehe Fault is closely linked, with no apparent geometric segmentation at the fault junction. Consequently, for earthquakes occurring on these faults, the seismic rupture can easily propagate through each other. This was evident in the map showing the distribution of intensities of the earthquake that occurred near Dongchuan on 2 August 1733 (Figure 1) (China Earthquake Administration, 1995). The surface rupture zone was located near Dongchuan but extended northward to Qiaojia without deviating toward Ningnan, indicating that the major earthquake near Dongchuan failed to propagate across the approximately 4.5 km wide Ningnan Basin and bend toward the Zemuhe Fault. Instead, it propagated through the junction between the northern segment of the Xiaojiang Fault and the Daliangshan Fault.

By studying the geometric patterns and kinematic characteristics of active faults in the area of intersection, the segmental features of seismic ruptures are analyzed, providing a basis for predicting the types and characteristics of strong earthquake disasters in cities along fault lines. The area of intersection of these faults poses a significant risk of major earthquakes. This area encompasses two counties, Ningnan County and Qiaojia County. Ningnan County is located primarily within the Ningnan pull-apart basin, with active faults distributed mainly on both sides of the basin and no apparent active faults traversing through the interior of the basin. With respect to strong earthquakes in this area in the future, attention should be given to the effect of amplification of thickly layered Quaternary deposits within the basin on strong ground motion, leading to structural damage in Ningnan County, but without the hazard of fault displacement or the need to address issues of active fault avoidance.

On the other hand, the town of Qiaojia is situated on an active fault, with many residential buildings and schools located along its course, necessitating active fault detection. Additionally, the northern segment of the Xiaojiang Fault has experienced severe landslide disasters, with multiple ancient landslides occurring in the area, among which the town of Qiaojia is located on one such ancient landslide body (Liu et al., 2022). Therefore, considering the avoidance of active faults in Qiaojia, the potential impact of landslide disasters must also be considered. With the completion and impoundment of the Baihetan hydropower station, the town of Qiaojia has undergone relocation and reconstruction, establishing multiple centralized residential resettlement communities primarily consisting of mid-rise and high-rise buildings. These resettlement communities are located relatively close to the reservoir, and any landslide disaster would result in significant losses and increase the difficulty of rescue efforts.

7 Conclusion

Through aerial photograph interpretation, field surveys, and seismic data analysis, research is conducted with respect to the geometric pattern, characteristics of movement, and segmentation of ruptures in the fault intersection zone of the Dalingshan–Zemuhe–Xiaojiang Fault from Ningnan to Qiaojia. This area experienced an extensional stress environment, with the three faults exhibiting left-lateral strike-slip movement combined with a dip-slip sense of movement. Moreover, the bend structure and the Ningnan Basin developed in the Ningnan–Qiaojia pull-apart zone. The Daliangshan Fault gradually intersects the Xiaojiang Fault near Qiaojia, and there is no obvious boundary of the fault segment between them.

With respect to severe earthquake events in the region, bends on the Xiaojiang Fault and the Ningnan pull-apart Basin are highly capable of impeding the propagation of seismic ruptures. Furthermore, due to the lack of prominent geometric barriers between the Dalingshan Fault and Xiaojiang Fault, the propagation of seismic ruptures during a great earthquake may have traversed both faults. Since active faults pass through urban areas of Qiaojia, it is vital to implement active fault detection in urban areas to guarantee safety.

Data availability statement

The original contributions presented in the study are included in the article/supplementary material, further inquiries can be directed to the corresponding author.

Author contributions

MW: Conceptualization, Investigation, Methodology, Writing–original draft, Writing–review and editing. ZW: Conceptualization, Writing–review and editing. FL: Conceptualization, Writing–review and editing. HC: Investigation, Writing–original draft. SL: Investigation, Writing–original draft.

Funding

Conflict of interest

The authors declare that the research was conducted in the absence of any commercial or financial relationships that could be construed as a potential conflict of interest.

Publisher's note

All claims expressed in this article are solely those of the authors and do not necessarily represent those of their affiliated organizations, or those of the publisher, the editors and the reviewers. Any product that may be evaluated in this article, or claim that may be made by its manufacturer, is not guaranteed or endorsed by the publisher.

References

Aki, K. (1984). Asperities, barriers, characteristic earthquakes and strong motion prediction. *J. Geophys. Res. Solid Earth* 89 (B7), 5867–5872. doi:10.1029/jb089ib07p05867

Allen, C. R., Luo, Z., Qian, H., Wen, X., Zhou, H., and Huang, W. (1991). Field study of a highly active fault zone: the Xianshui River fault of southwestern China. *Geol. Soc. Am. Bull.* 103 (9), 1178–1199. doi:10.1130/0016-7606(1991)103<1178:FSOAHA>2.3.CO;2

Andrews, D. J. (1994). Fault geometry and earthquake mechanics. *Ann. Geophys.* 6, 1341–1348. doi:10.4401/ag-4136

Bai, M., Chevalier, M.-L., Pan, J., Anne, R., Hervé, L. P., Marianne, M., et al. (2018). Southeastward increase of the late Quaternary slip-rate of the Xianshuihe fault, eastern Tibet. Geodynamic and seismic hazard implications. *Earth Planet. Sci. Lett.* 485, 19–31. doi:10.1016/j.epsl.2017.12.045

Chen, G., Xu, X., Wen, X., and Wang, Y. (2008). Kinematical transformation and slip par-titioning of northern to eastern active boundary belt of Sichuan–Yunnan block. *Seismol. Geol.* 30, 58–85. (in Chinese).

Chevalier, M. L., Leloup, P. H., Replumaz, A., Pan, J., Metois, M., and Li, H. (2017). Temporally constant slip-rate along the Ganzi fault, NW Xianshuihe fault system, eastern Tibet. *Geol. Soc. Am. Bull.* 130, 396–410. doi:10.1130/B31691.1

China Earthquake Administration (1995). *Catalogue of Chinese historical strong earthquakes [M]*. Beijing: Seismological Press. (in Chinese).

Duan, B., and Oglesby, D. D. (2005). Multicycle dynamics of nonplanar strike-slip faults. *J. Geophys. Res. Solid Earth* 110, B3. doi:10.1029/2004jb003298

Duman, T. Y., and Emre, Ö. (2013). The East Anatolian Fault: geometry, segmentation and jog characteristics. *Geol. Soc. Lond. Spec. Publ.* 372 (1), 495–529. doi:10.1144/sp372.14

Hamling, I. J., Hreinsdóttir, S., Clark, K., Elliott, J., Liang, C., Fielding, E., et al. (2017). Complex multifault rupture during the 2016 Mw 7.8 Kaikōura earthquake, New Zealand. *Science* 356 (6334), eaam7194. doi:10.1126/science.aam7194

Han, Z., Dong, S., Mao, Z., Hu, N., Tan, X., Yuan, R., et al. (2017). The Holocene activity and strike-slip rate of the southern segment of Xiaojiang fault in the southeastern Yunnan region, China. *Seismol. Geol.* 39 (1), 1–19. (in chinese). doi:10.3969/j.issn.0253-4967.2017.01.001

Harris, R. A., and Day, S. M. (1993). Dynamics of fault interaction: parallel strike-slip faults. *J. Geophys. Res. Solid Earth* 98 (B3), 4461–4472. doi:10.1029/92jb02272

He, H., Ikeda, Y., Song, F., and Dong, X. (2002). Late Quaternary slip rate of the Xiaojiang fault and its implication. *Seismol. Geol.* 24, 14–26.

He, H., Song, F., and Chuanyou, Li (1999). Topographic survey of micro faulted landform and estimation of strike slip rate for the Zemuhe Fault, sichuan Province. *Seismol. Geol.* 21 (4), 361–369. (in chinese).

He, H., Ikeda, Y., He, Y. L., Togo, M., Chen, J., Chen, C. Y., et al. (2008). Newly generated Daliangshan fault zone — shortcutting on the central section of Xianshuihe-Xiaojiang fault system. *Sci. China (Series D)* 51 (9), 1248–1258. doi:10.1007/s11430-008-0094-4

Jia, Z., Jin, Z., Marchandon, M., Ulrich, T., Gabriel, A., Fan, W., et al. (2023). The complex dynamics of the 2023 Kahramanmaraş, Turkey, Mw 7.8-7.7 earthquake doublet. *Science* 381, 985–990. eadi0685. doi:10.1126/science.adi0685

Kame, N., Rice, J. R., and Dmowska, R. (2003). Effects of prestress state and rupture velocity on dynamic fault branching. *J. Geophys. Res. Solid Earth* 108 (B5). doi:10.1029/2002jb002189

Kissling, E. (1988). Geotomography with local earthquake data. *Rev. Geophys* 26 (4), 659–698. doi:10.1029/rg026i004p00659

Kissling, E., Ellsworth, W., Eberhart-Phillips, D., and Kradolfer, U. (1994). Initial reference models in local earthquake tomography. *J. Geophys Res.* 99, 19635–19646. doi:10.1029/93jb03138

Kissling, E., Kradolfer, U., and Maurer, H. (1995). VELEST userES guideshort introduction. *Tech. rep. Inst. Geophys. ETH Zurich, kiss@tomo.ig.erdw.ethz.ch*.

Klein, F. W. (1989) *HYPOINVERSE, a program for VAX computers to solve for earthquake locations and magnitudes*, 89-314. U.S. Geological Survey Open-File Report, 59.

Liu, Li, Zhang, L., Li, P., Yang, X., and Deng, Q. (2022). Development characteristics and formation conditions of the giant ancient landslide along Qiaojia segment of Jinshajiang river. *Yangtze River* 53 (1), 118–125. (in chinese).

Long, F., Wen, X. Z., Ruan, X., Zhao, M., and Yi, G. X. (2015). A more accurate relocation of the 2013 M S 7.0 Lushan, Sichuan, China, earthquake sequence, and the seismogenic structure analysis. *J. Seismol.* 19, 653–665. doi:10.1007/s10950-015-9485-0

Loveless, J. P., and Meade, B. J. (2011). Partitioning of localized and diffuse deformation in the Tibetan Plateau from joint inversions of geologic and geodetic observations. *Earth Planet. Sci. Lett.* 303 (1), 11–24. doi:10.1016/j.epsl.2010.12.014

Lozos, J. C., Oglesby, D. D., Duan, B., and Wesnousky, S. G. (2011). The effects of double fault bends on rupture propagation: a geometrical parameter study. *Bull. Seismol. Soc. Am.* 101 (1), 385–398. doi:10.1785/0120100029

Nielsen, S. B., and Knopoff, L. 1998. The equivalent strength of geometrical barriers to earthquakes. *J. Geophys. Res. Solid Earth*, 103(B5), 9953–9965. doi:10.1029/97jb03293

Ran, Y, Chen, J, Gong, H, and Chen, L 2008. Late Quaternary geomorphic deformation and displacement rates of the Anninghe fault around Zimakua. *Seismol. Geol.* 30 (1), 86–98.

Ren, J., and Ping, Li (1989). Research on seismic landforms and paleoearthquakes in the north segment of the Zemuhe Fault Zone. *Seismol. Geol.* 11 (1), 27–34. (in chinese).

Rongjun, Z., Xiaogang, Li, Huang, Z., He, Y., and Ge, T. (2003). Average slip rate of daliangshan Fault Zone in sichuan in late quaternary period. *J. Seismol. Res.* 26 (2), 191–196. (in chinese).

Shao, Y., Liu-Zeng, J., Oskin, M. E., Elliott, A. J., Wang, P., Zhang, J., et al. (2018). Paleoseismic investigation of the Aksay restraining double bend, Altyn Tagh fault, and its implication for barrier-breaching ruptures. *J. Geophys. Res. Solid Earth* 123, 4307–4330. doi:10.1029/2017jb015397

Shen, Z.-K., Lü, J., Wang, M., and Bürgmann, R. (2005). Contemporary crustal deformation around the southeast borderland of the Tibetan Plateau. *J. Geophys. Res. Solid Earth* 110 (B11). doi:10.1029/2004jb003421

Sieh, K., Jones, L., Hauksson, E., Hudnut, K., Eberhart-Phillips, D., Heaton, T., et al. (1993). Near-field investigations of the landers earthquake sequence, april to july 1992. *Science* 260 (5105), 171–176. doi:10.1126/science.260.5105.171

Song, F., Yipeng, W., Weixian, Yu, Cao, Z., and Shen, X. (1998). *Shen Jun. Xiaojiang active fault zone*. Beijing: Seismology Press, 1–237. (in chinese).

Sun, H., He, H., Ikeda, Y., Wei, Z., Chen, C., Xu, Y., et al. (2019). Paleoearthquake history along the southern segment of the daliangshan Fault Zone in the southeastern Tibetan plateau. *Tectonics* 38 (7), 2208–2231. doi:10.1029/2018tc005009

Tapponnier, P., and Molnar, P. (1977). Active faulting and tectonics in China. *J. Geophys. Res.* 82 (20), 2905–2930. doi:10.1029/jb082i020p02905

Waldhauser, F., and Ellsworth, W. L. (2000). A double-difference earthquake location algorithm: method and application to the northern Hayward fault. *Bull. Seismol. Soc. Am.* 90, 1353–1368. doi:10.1785/0120000006

Wang, E., Burchfiel, B. C., and Burchfiel, B. C. (2000). Late Cenozoic to Holocene deformation in southwestern Sichuan and adjacent Yunnan, China, and its role in formation of the southeastern part of the Tibetan Plateau. *GSA Bull.* 112 (3), 413–423. doi:10.1130/0016-7606(2000)112<413:lcthdi>2.0.co;2

Wang, E., Burchfiel, B. C., Royden, L. H., Chen, L. Z., Chen, J. S., Li, W. X., et al. (1998). *Late cenozoic xianshuihe-xiaojiang, Red River, and dali fault systems of southwestern sichuan and central yunnan*. China: Geological Society of America.

Wang, W., Qiao, X., and Ding, K. (2021). Present-day kinematics in southeastern tibet inferred from GPS measurements. *J. Geophys. Res. Solid Earth* 126 (1), e2020JB021305. doi:10.1029/2020jb021305

Wen, X. (1983). Model of active tectonic of the Quaternary period of Zemu river fault. *J. Seismol. Res.* 6 (1), 41–50. (in chinese).

Wen, X. (2000). Segmentation characteristics of earthquake rupture in the xianshuihe-anninghe-zemuhe fault zone in western sichuan. *Seismol. Geol.* 22 (3), 239–249. (in chinese).

Wen, X., Ma, S., Xu, X., and He, Y. (2008). Historical pattern and behavior of earthquake ruptures along the eastern boundary of the Sichuan-Yunnan faulted-block, southwestern China. *Phys. Earth Planet. Interiors* 168 (1–2), 16–36. doi:10.1016/j.pepi.2008.04.013

Wesnousky, S. G. (2006). Predicting the endpoints of earthquake ruptures. *Nature* 444 (7117), 358–360. doi:10.1038/nature05275

Wesnousky, S. G. (2008). Displacement and geometrical characteristics of earthquake surface ruptures: issues and implications for seismic-hazard analysis and the process of earthquake rupture. *Bull. Seismol. Soc. Am.* 98 (98), 1609–1632. doi:10.1785/0120070111

Xu, X, Wen, X, Zheng, R, Ma, W., Song, F., and Yu, G. (2003). Pattern of latest tectonic motion and its dynamics for active blocks in Sichuan-Yunnan region, China. *Sci. China(Ser D)* 46 (Suppl), 210–226. doi:10.1360/03dz0017

Yi, G., Long, F., Liang, M., Zhao, M., Zhang, H., Zhou, R., et al. (2023). Seismogenic structure of the 5 september 2022 sichuan luding Ms6.8 earthquake sequence. *Chinese. J. Geophys.* 66 (4), 1363–1384. (in chinese). doi:10.6038/cjg2023Q0923

Zhang, P. Z. (2013). A review on active tectonics and deep crustal processes of the western Sichuan region, eastern margin of the Tibetan Plateau. *Tect.* 584, 7–22. doi:10.1016/j.tecto.2012.02.021

Zhanyu, W., He, H., Feng, S., Yueren, Xu, Bi, L., and Sun, H. (2012). Estimation of slip rate on the south segment of daliangshan Fault Zone. *Seismol. Geol.* (2), 282–293. (in chinese).

Zhu, Z., and Zhang, R. S. (1987). The compilation of regional travel time table in Sichuan. *Earthq. Res. Sichuan* 1987 (2), 29–35. (in Chinese with English abstract).